FAM122B acts as an independent poor prognostic factor and promotes the malignant biological behaviors of low-grade glioma

HAO WANG[1,2*], TENGFEI GUO[2*], YANBO GAO[2*], YI ZHOU[1] and RONGJUN QIAN[2]

[1]The First Affiliated Hospital of Henan University of Chinese Medicine, Zhengzhou, Henan 450003, P.R. China;
[2]Department of Neurosurgery, Henan Provincial People's Hospital, Zhengzhou, Henan 450003, P.R. China

Received February 25, 2026; Accepted June 16, 2026

DOI: 10.3892/ol.2026.15782

Abstract. The aim of the present study was to investigate the role and mechanism of Family with sequence similarity 122, member B (*FAM122B*) in low-grade glioma (LGG) by combining bioinformatics analysis of public databases and *in vitro* cell experiments. Data from databases including Gene Expression Omnibus, The Cancer Genome Atlas and Chinese Glioma Genome Atlas were integrated to analyze the expression characteristics, clinical correlations and molecular mechanisms of *FAM122B*. Meanwhile, SHG44 cells were used as the research object and short interfering RNA was applied to knockdown *FAM122B* expression to verify its effects on cell functions. The results showed that *FAM122B* was markedly highly expressed in LGG tissues and cell lines compared with normal brain tissues and normal glial cells, which was closely associated with the malignant clinical features of LGG. Patients with high *FAM122B* expression had a poorer prognosis, and *FAM122B* was identified as an independent adverse prognostic marker for LGG. *In vitro* experiments confirmed that knockdown of *FAM122B* could markedly inhibit the proliferation and migration of SHG44 and SW1088 cells. In conclusion, *FAM122B* plays a key oncogenic role in LGG and it was hypothesized to serve as a potential biomarker for prognostic evaluation and a novel target for the targeted therapy of LGG, providing a theoretical basis for its precise diagnosis and treatment.

Introduction

The Cancer Genome Atlas (TCGA) defines patients with World Health Organization (WHO) grade II or III glioma as low-grade glioma (LGG) (1), which accounts for 20-40% of all glioma cases (2). The cumulative risk of progression to glioblastoma (GBM) within a 10-year follow-up period is ~70% (3), posing a severe threat to the life and health of patients. Current treatment strategies are mainly based on surgical resection combined with neoadjuvant therapies such as radiotherapy and chemotherapy, yet the postoperative recurrence rate remains considerably high (4). With the advance of next-generation sequencing technology, a large number of tumor-associated molecular biomarkers have been identified and gradually applied in clinical practice, providing a novel direction for the precise diagnosis and treatment of tumors (5). Although GBM exhibits higher malignancy, genomic expression disorders frequently occur during tumorigenesis and progression, and the molecular mechanisms underlying such disorders often differ between GBM and LGG (6). Therefore, the present study focused on LGG to screen molecular biomarkers associated with disease progression, laying a theoretical foundation for subsequent combined therapy for LGG.

Family with sequence similarity 122 (FAM122) is a class of highly conserved proteins (7), whose members include *FAM122A*, *FAM122B* and *FAM122C*. *FAM122A* is the most extensively studied member of the family and has been identified as a key negative regulator of the protein phosphatase 2A (*PP2A*) holoenzyme (8). *FAM122A* can specifically bind to the interaction interface between the scaffold subunit Aα and the regulatory subunit B55α through its conserved domain, directly impairing the assembly stability of the PP2A/Aα-B55α-C holoenzyme, thereby inhibiting the phosphatase activity of PP2A (9). This inhibitory effect leads to hyperphosphorylation and stable expression of downstream oncoproteins (such as MYC), ultimately promoting abnormal cell cycle progression, inhibiting apoptosis and enhancing the invasive and proliferative capacities of tumor cells (10). For instance, *FAM122A* has been confirmed to promote the progression of acute myeloid leukemia by modulating the expression of PP2A and MYC (10). In addition, in hepatocellular carcinoma, *FAM122A* can regulate PP2A-dependent downstream pathways to facilitate cancer cell growth and increase chemoresistance to doxorubicin (11).

In contrast to the well-characterized *FAM122A*, the physiological functions and pathological mechanisms of *FAM122B* remain to be fully elucidated to date. As a homologous protein of *FAM122A*, *FAM122B* may also possess similar oncogenic

Correspondence to: Dr Rongjun Qian, Department of Neurosurgery, Henan Provincial People's Hospital, 7 Weiwu Road, Jinshui, Zhengzhou, Henan 450003, P.R. China
E-mail: doctorqianrongjun@163.com

*Contributed equally

Key words: low-grade glioma, *FAM122B*, prognostic biomarker, oncogene, cell proliferation

potential. In the preliminary stage of the present study, differential analysis revealed that *FAM122B* is highly expressed in LGG, suggesting its potential correlation with the malignant phenotype of tumors. The present study aimed to clarify whether *FAM122B* is involved in regulating the proliferative capacity of LGG cells and its role in the malignant progression of the disease, thereby providing a reference for the subsequent development of diagnostic and therapeutic targets.

Materials and methods

Cell culture. All the cell lines used in the present study (HA1800, SHG44 and SW1088) were purchased from TongPai (Shanghai) Biotech Co., Ltd. The HA1800 cells (cat. no. HA1800; http://www.shtpbio.com/tongpai-Products/) used in the present study were immortalized human normal astrocytes. HA1800 and SHG44 cells were cultured in high-glucose DMEM medium (Cytiva; cat. no. SH30022), while SW1088 cells were maintained in Leibovitz L-15 medium (Cytiva; cat. no. SH30525). All media were supplemented with 10% fetal bovine serum (HySigen Biosciences; cat. no. FBP-S005) and 1% penicillin-streptomycin solution (Beijing Solarbio Science & Technology Co, Ltd.; cat. no. P1400) to sustain cell growth and inhibit microbial contamination. The cells were incubated in a constant-temperature cell incubator at 37˚C with 5% CO_2 and saturated humidity. Cell density was observed daily. When the cell confluence reached ~90%, the cells were rinsed twice with phosphate-buffered saline (Beijing Solarbio Science & Technology Co, Ltd.; cat. no. P1020), followed by digestion into single-cell suspension using 0.25% trypsin-EDTA (Beijing Solarbio Science & Technology Co, Ltd.; cat. no. T1300). The digestion was terminated with complete medium prior to subsequent treatments.

Cell transfection. SHG44 and SW1088 cells were seeded at a density of $5x10^5$ cells/well into 6-well cell culture plates (Wuhan Servicebio Technology Co., Ltd.; cat. no. CCP-6H) and cultured at 37˚C overnight until cell confluence reached 50-60%. After which, cells were treated with the transfection reagent, Lipofectamine® 3000 (Thermo Fisher Scientific, Inc.; cat. no. L3000075), and the transfection medium, Opti-MEM™ I Reduced Serum Medium (Thermo Fisher Scientific, Inc.; cat. no. 31985070). Small interfering RNA (siRNA) targeting *FAM122B* was purchased from Shanghai GenePharma Co., Ltd. The sequences of *FAM122B* siRNA were sense strand: 5'-CGG AGGAATAGTACAACAATTdTdT-3', antisense strand: 5'-AAT TGTTGTACTATTCCTCCGdTdT-3' (RefSeq accession number: NM_145284). The sequences of negative control siRNA were sense strand: 5'-UUCUCCGAACGUGUCACGUdTdT-3', antisense strand: 5'-ACGUGACACGUUCGGAGAAdTdT-3'. The final working concentration of siRNA for cell transfection was 50 nM. For transfection, *FAM122B* siRNA and Lipofectamine® 3000 reagent were separately diluted in Opti-MEM Reduced Serum Medium, allowed to stand for 5 min, gently mixed and incubated at room temperature for 20 min to form stable transfection complexes. Subsequently, the transfection complexes were slowly added dropwise into 6-well plates containing reduced serum medium. After 6-8 h of transfection, the medium was replaced with complete medium and cell culture was continued.

Reverse transcription-quantitative (RT-q)PCR. The cells were seeded at a confluency of 60-70%. At 24-48 h post-transfection, total RNA was extracted from LGG cells using an RNA extraction kit (Omega Bio-Tek, Inc.; cat. no. R6834). The concentration and purity of RNA were measured by Thermo Fisher NanoDrop micro-spectrophotometer (Thermo Fisher Scientific, Inc.). After which, the extracted RNA was reverse-transcribed into cDNA using a reverse transcription kit (Novoprotein Scientific Co., Ltd.; cat. no. E047) under the following conditions: 25˚C for 5 min, 50˚C for 15 min and 85˚C for 5 min, with final storage at 4˚C. qPCR was performed using a qPCR kit (Novoprotein Scientific Co., Ltd.; cat. no. E096) to verify transfection efficiency with the following conditions: Pre-denaturation at 95˚C for 5 min for 1 cycle; 95˚C for 10 sec and 60˚C for 30 sec for a total of 40 cycles. Primer sequences were as follows: *FAM122B* (alias *PABIR2*) forward primer, AAGGGAAATGCAAACGGCAAT and reverse primer, TCTCCGGCTTGTCAAAATCAC; 18S forward primer, CACCAGACTTGCCCTCCAAT and reverse primer, CCT GAGAAACGGCTACCACAT. All primers were obtained from Zhengzhou Shangzhiya Biotechnology Co., Ltd. RNA extraction, cDNA synthesis and qPCR were performed strictly in accordance with the manufacturer's protocols. The $2^{-\Delta\Delta Cq}$ method was used to calculate relative gene expression levels (12), and all aforementioned experiments were repeated in triplicate. Under the experimental conditions used in this study, 18S was stably expressed, with no significant differences in C^q values between the NC and siRNA groups.

CCK-8 cell proliferation assay. Transfected SHG44 and SW1088 cells were seeded in 96-well plates at a density of $2x10^3$ cells/well, with 6 replicate wells set for each group to reduce experimental errors. Assays were performed at the following five time points: 0, 24, 48, 72 and 96 h post-seeding. Specifically, 10 μl CCK-8 reagent (Shanghai Saint-Bio Biotechnology Co., Ltd.; cat. no. ST1008) was added to each well, and the plate was gently shaken to ensure thorough mixing of the reagent with the medium. The plate was then incubated at 37˚C for 1 h in the dark. After incubation, a microplate reader was used to measure the absorbance (OD value) of each well at a wavelength of 450 nm, with the OD value serving as an indicator of cell proliferation activity.

Colony formation assay. Transfected SHG44 and SW1088 cells were digested into a single-cell suspension, counted and uniformly seeded in 6-well plates at a density of 1,000 cells/well, with three replicate wells set up for each group. The cells were cultured for 10-15 days, with the medium replaced every three days. After visible cell clones formed, the medium was discarded, and the cells were fixed with 4% paraformaldehyde at room temperature for 30 min, followed by staining with 0.1% crystal violet solution at room temperature for a further 30 min. Excess dye was rinsed off with running water, and the plates were air-dried. Cell colonies were defined as cell clusters with a size of >100 $pixel^2$ and analyzed using ImageJ software (version 1.54i; National Institutes of Health).

Wound healing assay. Transfected SHG44 and SW1088 cells were seeded in 6-well plates and cultured until >90% confluence. A horizontal line was drawn on the back of each 6-well

plate as an anchor point to ensure consistent imaging fields at all time points. A straight scratch wound was made vertically across the horizontal line at the center of each well using a sterile 1,000 μl pipette tip, with effort made to maintain uniform wound width across all wells. The cells were rinsed twice with PBS to remove floating cells, and the medium was replaced with serum-free medium. Images of the wound areas were captured under an inverted microscope at 0, 24 and 48 h post-scratching, respectively. The wound healing rate was calculated using Image software (version 1.54i, National Institutes of Health) according to the following formula: Wound healing rate=[(wound width at 0 h-wound width at 24/48 h)/wound width at 0 h] x100%. This index was used to evaluate the migratory ability of the cells.

Transwell assay. Cell migration ability was assessed using uncoated Transwell chambers (Wuhan Servicebio Technology Co., Ltd.; cat. no. WG3415). Transfected SHG44 and SW1088 cells were digested into a single-cell suspension, resuspended in serum-free medium and adjusted to a density of $1x10^5$ cells/ml. A 200 μl aliquot of the cell suspension was added to the upper chamber, while 600 μl complete medium was placed in the lower chamber as a chemoattractant. After incubation at 37˚C for 24 h, non-migratory cells on the upper surface of the chamber membrane were gently wiped off with cotton swabs. Migratory cells on the lower surface were fixed with 4% paraformaldehyde (Wuhan Servicebio Technology Co., Ltd.; cat. no. P1110) at room temperature for 30 min and stained with 0.1% crystal violet solution (Wuhan Servicebio Technology Co., Ltd.; cat. no. C8470) at room temperature for a further 30 min. Excess dye on the membrane surface was rinsed away slowly with running water, followed by air-drying at room temperature. Images were captured under an inverted microscope for cell counting, and the average number of migratory cells was calculated to evaluate cell migration ability.

Data collection. Several public databases and datasets were employed for bioinformatics analyses. Firstly, gene expression profiles were retrieved from five publicly available Gene Expression Omnibus (GEO) datasets (https://www.ncbi.nlm.nih.gov/geo/) (dataset nos. GSE35493, GSE43378, GSE50025, GSE74187 and GSE83300), with detailed characteristics of these datasets presented in Table SI. TCGA (https://portal.gdc.cancer.gov/) database provided mRNA sequencing data and corresponding clinical information of 503 LGG cases, and the Chinese Glioma Genome Atlas (CGGA) database (http://www.cgga.org.cn/) included 403 cases of mRNA sequencing data, 142 cases of microarray data and matched clinical characteristics of LGG. In addition, the Human Protein Atlas (HPA) database (https://www.proteinatlas.org/), contained immunohistochemistry (IHC) data of *FAM122B* in three normal cerebral cortex samples and five LGG tissue samples. Finally, the TIMER database (TIMER2.0; https://cistrome.shinyapps.io/timer/) supplied immune cell infiltration data of LGG tissues. All data were downloaded from the official websites of the corresponding databases. The inclusion criteria were complete mRNA expression data and available clinical follow-up information.

Gene set enrichment analysis (GSEA). To explore the potential molecular pathways through which high *FAM122B* expression regulates LGG progression, GSEA was performed using GSEA software (version 4.3.3; https://www.gsea-msigdb.org/gsea/index.jsp). The gene set employed for analysis was c2.cp.v7.5.symbols.gmt (pathway-associated gene set), which was used to assess the enrichment levels of pathways between the *FAM122B* high-expression group and low-expression group. Pathways with a false discovery rate (FDR) <0.25 and P<0.05 were defined as markedly enriched pathways.

Meta-analysis. For retrospective studies, meta-analysis can integrate and pool multiple datasets from different sources, thereby improving the generalizability and extrapolation of research conclusions. Previous findings of the present study indicated that high expression of *FAM122B* serves as an adverse prognostic risk factor in LGG. To further expand the sample size and verify whether the negative effect of *FAM122B* expression on the prognosis of patients with LGG is universally applicable, the following seven independently sourced datasets were included in the present study: i) TCGA RNA-Seq (https://portal.gdc.cancer.gov/); ii) CGGA mRNA-array (http://www.cgga.org.cn/); iii) CGGA RNA-Seq; iv) GSE43378 (13); v) GSE50025 (14); vi) GSE74187 (15); and vii) GSE83300 (16) (https://www.ncbi.nlm.nih.gov/geo/). The aforementioned datasets cover cohorts from different countries and ethnic populations, and adopt multiple molecular detection platforms. Prior to conducting the meta-analysis, a separate prognostic analysis was performed for each dataset. The Cox regression model was used to obtain the prognostic effect sizes of each cohort, followed by meta-analysis to pool and synthesize these prognostic effect sizes across all studies. The present study used the I^2 statistic to assess the heterogeneity among datasets. Statistical analyses were conducted using R software (version 4.5.0; R Foundation for Statistical Computing; https://www.r-project.org/) and the 'meta' (https://CRAN.R-project.org/package=meta) package. Significant statistical heterogeneity was defined as I^2>50% accompanied by P<0.05 for the heterogeneity test. A random-effects model was used for pooled analyses to account for potential between-study heterogeneity.

Statistical analysis. Statistical analyses and visualizations were performed using R software (version 4.5.0) with the 'survival' (https://CRAN.R-project.org/package=survival), 'survminer' (https://CRAN.R-project.org/package=survminer), 'corrplot' (https://CRAN.R-project.org/package=corrplot), 'ggplot2' (https://CRAN.R-project.org/package=ggplot2), 'dplyr' (https://CRAN.R-project.org/package=dplyr), 'pROC' (https://CRAN.R-project.org/package=pROC) and 'forestplot' (https://CRAN.R-project.org/package=forestplot) packages. A two-tailed significance level was set at α=0.05, with P<0.05 considered to indicate a statistically significant difference. First, data on target gene expression, clinicopathological characteristics and survival outcomes (endpoint events, follow-up time and censoring status) of the study samples were collated. After quality control, samples were divided into high and low expression groups based on the median value of gene expression. For clinical correlation analysis, Pearson/Spearman correlation analyses were used for continuous variables, and χ^2 test was applied for categorical variables. Kaplan-Meier curves were plotted to visualize survival distributions, and

the Log-rank test was used to compare survival differences between the high and low gene expression groups. Univariate and multivariate Cox proportional hazards regression analyses were sequentially conducted. After verifying the proportional hazards assumption via the Schoenfeld residual method, independent risk factors for survival outcomes were identified, with hazard ratio (HR) and 95% confidence interval (CI) calculated, and forest plots generated to present the results. The 'ROC' package was used to plot receiver operating characteristic (ROC) curves and calculate the area under the curve (AUC) for evaluating the predictive value of target gene expression for clinical outcomes of the subjects. All experimental data were statistically analyzed using GraphPad Prism 10.0 software (Dotmatics). Student's t-test was used for comparisons between two groups, while one-way ANOVA followed by Dunnett's multiple comparisons test was applied for datasets with three or more groups. Quantitative data were expressed as mean ± standard deviation. Survival data were displayed via Kaplan-Meier survival curves. Correlation results were presented in correlation heatmaps. HR results were visualized by forest plots. Diagnostic efficacy was shown by ROC curves. Enumeration data were presented as case numbers and percentages.

Results

Expression analysis of FAM122B in LGG. Malignant progression of gliomas is often accompanied by disorders of genomic expression profiles (17). To clarify the expression characteristics of *FAM122B* in gliomas, the present study first performed bioinformatics analysis using the GSE35493 dataset from the GEO database. The results showed that the mRNA level of *FAM122B* was markedly higher in tumor tissues than in normal brain tissues (normal group, n=9; tumor group, n=12; Fig. 1A). To verify the aforementioned bioinformatics analysis results, the mRNA expression level of *FAM122B* in LGG cell lines and normal astrocytes was detected using the RT-qPCR assay. The human normal astrocyte cell line HA1800 was selected as the control, and the LGG cell lines SW1088 and SHG44 were used as the research objects. The results confirmed that the mRNA of *FAM122B* was markedly higher in LGG cell lines than in normal HA1800 glial cells (Fig. 1B), which was consistent with the database analysis results. Furthermore, the expression difference of *FAM122B* was verified at the protein level. The IHC data for *FAM122B* were retrieved from the HPA database, and downloaded and analyzed the IHC results of three cases of normal cerebral cortex tissues and five cases of LGG tumor tissues (Figs. 1D and E; S1 and S2). The results showed that compared with normal cerebral cortex tissues, the protein expression level of *FAM122B* in LGG tumor tissues was markedly increased (Fig. 1C). The results of the present study demonstrated that *FAM122B* is highly expressed at both the mRNA and protein levels in LGG tissues and cell lines, which lays an experimental foundation for the subsequent in-depth exploration of the correlation between the high expression of *FAM122B* and the poor prognosis of patients with LGG.

Analysis of the correlation between FAM122B expression and clinical characteristics of patients with LGG. To explore the correlation between *FAM122B* expression and the clinical characteristics of patients with LGG, mRNA expression data and corresponding clinical characteristic information from patients with LGG were downloaded from three databases, namely TCGA-seq, CGGA-seq and CGGA microarray, and an integrated analysis was performed. Firstly, in terms of clinical grading, the prognosis of patients with WHO grade III LGG was markedly worse than that of patients with WHO grade II (18). Meanwhile, in all three aforementioned databases, it was observed that the mRNA expression level of *FAM122B* was markedly upregulated with increasing WHO grade of gliomas (Fig. 2A-C), suggesting a positive correlation between its expression and the malignant degree of tumors. Second, compared with primary LGG, recurrent LGG tumor cells possess stronger invasiveness and lead to worse prognosis (19). Data from three databases indicated that the mRNA expression level of *FAM122B* was higher in samples from recurrent patients than in those from primary patients (Fig. 2D-F). Finally, analysis of key molecular markers based on glioma grading showed that IDH mutation and 1p19q chromosome co-deletion are important indicators of favorable prognosis in patients with LGG (20). Meanwhile, the mRNA expression level of *FAM122B* in tumor tissues was correspondingly decreased in patients with LGG with IDH mutation (Fig. 2G and H) and 1p19q co-deletion (Fig. 2I) phenotypes, which further confirmed that *FAM122B* expression is correlated with the prognostic characteristics of patients. In summary, the results of multi-database and multi-clinical dimension analyses all indicate that high *FAM122B* expression is closely correlated with malignant clinical phenotypes of patients with LGG (high grade, recurrence, absence of IDH mutation and non-co-deletion of 1p19q), suggesting that its high expression may drive the deterioration of clinical prognosis in patients with LGG. Based on these results, the direct correlation between *FAM122B* expression level and the prognosis of patients with LGG will be further explored in subsequent studies.

FAM122B is a potential prognostic marker for LGG. Survival time is one of the core direct indicators for evaluating the prognosis of patients with tumors. To clarify the direct correlation between *FAM122B* expression level and the prognosis of patients with LGG, the survival time and survival status information of all patients with LGG were extracted from the three aforementioned databases, the patients were divided into high-expression and low-expression groups according to the mRNA expression level of *FAM122B*, and survival prognosis analysis was conducted. First, KM survival curve analysis was performed. The results showed that in the three databases of TCGA-seq, CGGA-seq and CGGA microarray, with the extension of follow-up time, the survival rate of patients in the *FAM122B* high-expression group was consistently lower than that in the low-expression group (Fig. 3A-C), and the differences between the groups were statistically significant (all $P<0.05$). Subsequently, the predictive value of *FAM122B* for the survival outcomes of patients with LGG was evaluated by ROC curve analysis. The results showed that in the three databases, the AUC of *FAM122B* for predicting the 1-, 3- and 5-year survival outcomes of patients was stably ~0.7 (Fig. 3D-F), suggesting that the short-term

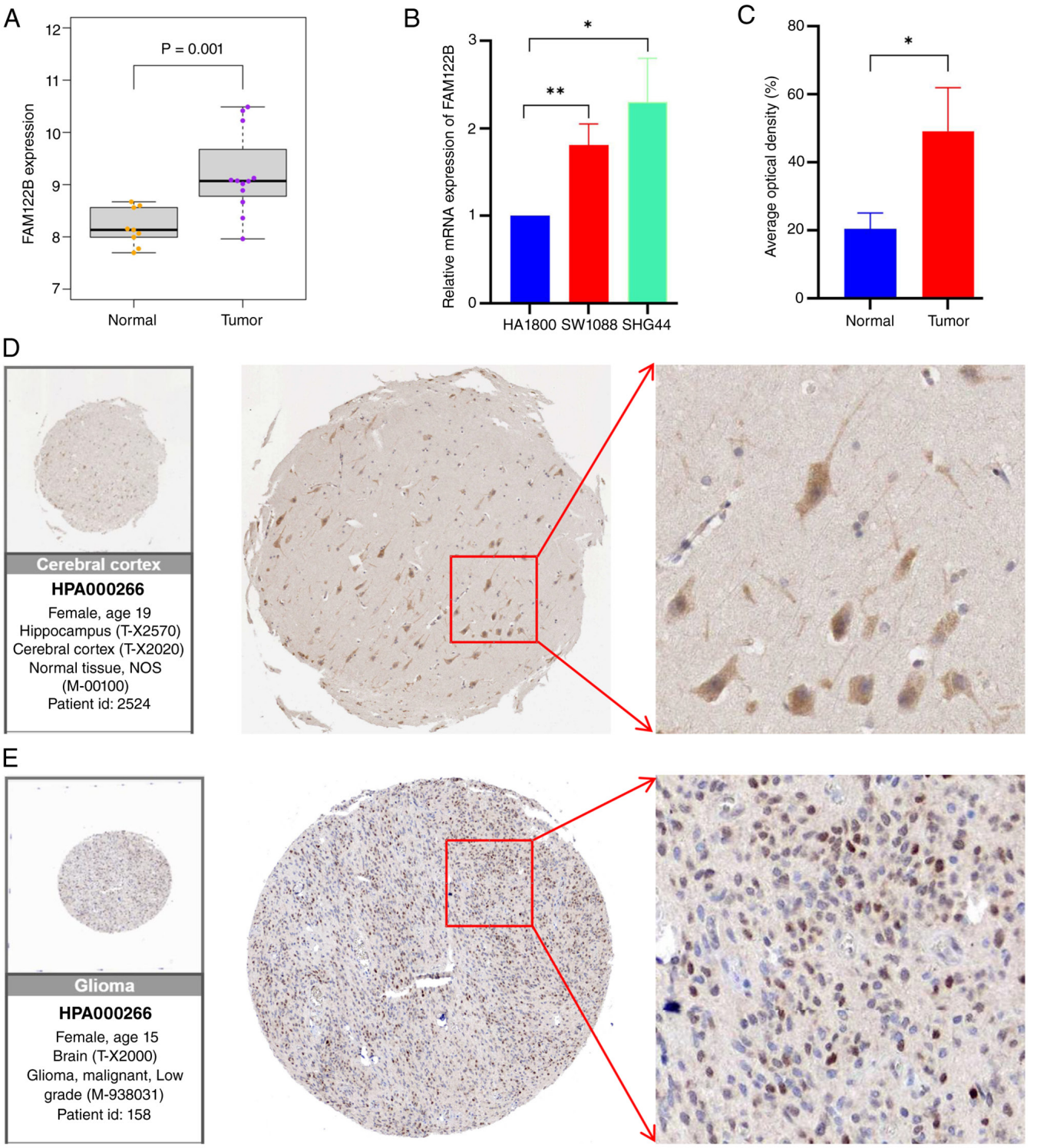

Figure 1. *FAM122B* is highly expressed in LGG tissues and cell lines. (A) mRNA expression levels of *FAM122B* in normal brain tissues (n=9) and LGG tumor tissues (n=12) from the GSE35493 dataset. (B) RT-qPCR results showing the relative mRNA expression of *FAM122B* in the human normal astrocyte cell line HA1800 and LGG cell lines SW1088 and SHG44. (C) Quantification of the IHC staining results in panels (D) and (E), showing the average optical density of *FAM122B* protein expression in normal cerebral cortex tissues (n=3) and LGG tumor tissues (n=5). Representative IHC staining image of *FAM122B* in (D) normal cerebral cortex tissues and (E) in LGG tumor tissues from the HPA database. All original magnification, x4.3. *P<0.05, **P<0.01. *FAM122B*, Family with sequence similarity 122, member B; LGG, low-grade glioma; RT-qPCR, reverse transcription-quantitative PCR; IHC, immunohistochemistry; HPA, Human Protein Atlas.

and medium-term survival prognosis of patients with LGG can be moderately predicted based solely on the expression level of *FAM122B*. Combined with the previous results on the correlation between high *FAM122B* expression and malignant clinical phenotypes of LGG, the survival analysis in this section further confirms that *FAM122B* is expected to serve as a molecular marker for evaluating the prognosis of patients with LGG.

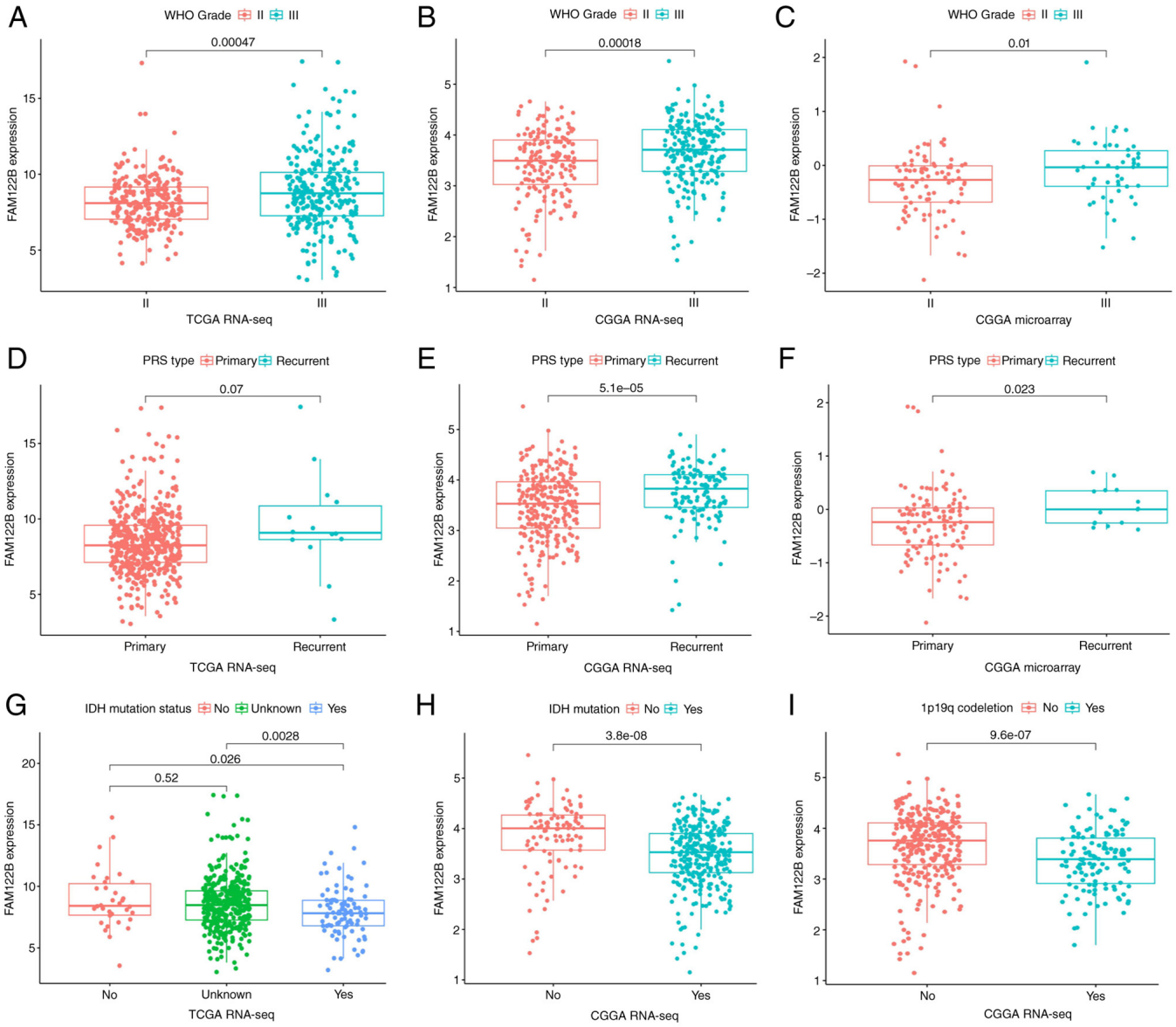

Figure 2. Correlation analysis between *FAM122B* expression level and clinicopathological characteristics of patients with LGG. (A) Comparison of *FAM122B* mRNA expression levels in LGG tissues with different WHO grades (grade II vs. grade III) based on TCGA RNA-seq dataset. (B) Comparison of *FAM122B* mRNA expression levels in LGG tissues with different WHO grades (grade II vs. grade III) based on CGGA RNA-seq dataset. (C) Comparison of *FAM122B* mRNA expression levels in LGG tissues with different WHO grades (grade II vs. grade III) based on CGGA microarray dataset. (D) Comparison of *FAM122B* mRNA expression levels between primary and recurrent LGG tissues in the TCGA RNA-seq dataset. (E) Comparison of *FAM122B* mRNA expression levels between primary and recurrent LGG tissues in the CGGA RNA-seq dataset. (F) Comparison of *FAM122B* mRNA expression levels between primary and recurrent LGG tissues in the CGGA microarray dataset. (G) Comparison of *FAM122B* mRNA expression levels in LGG tissues with different IDH mutation statuses based on TCGA RNA-seq dataset. (H) Comparison of *FAM122B* mRNA expression levels in LGG tissues with different IDH mutation statuses based on CGGA RNA-seq dataset. (I) Comparison of *FAM122B* mRNA expression levels in LGG tissues with different 1p19q co-deletion statuses based on the CGGA RNA-seq dataset. *FAM122B*, Family with sequence similarity 122, member B; LGG, low-grade glioma; WHO, World Health Organization; TCGA, The Cancer Genome Atlas; CGGA, Chinese Glioma Genome Atlas.

FAM122B is an independent poor prognostic factor for patients with LGG. Although the aforementioned ROC curve analysis clarified the predictive ability of *FAM122B* expression for the survival outcomes of patients with LGG, this analysis failed to exclude the potential confounding interference of clinical indicators such as age, pathological features and tumor stage, making it difficult to confirm its independent prognostic value. Therefore, the present study further adopted univariate and multivariate Cox proportional hazards regression models to clarify whether high *FAM122B* expression remains an independent risk factor for poor prognosis in patients with LGG after adjusting for the aforementioned confounding factors. Firstly, univariate Cox proportional hazards regression analysis was performed on samples from the three databases separately to rapidly screen for indicators with significant impacts on patient survival. The results showed that *FAM122B* expression level, age, WHO grade and tumor recurrence status were all significant factors affecting the prognosis of patients with LGG (all HR>1; P<0.05; Fig. 4A, C and E). Subsequently, these factors were incorporated into a multivariate Cox proportional hazards regression analysis to adjust for the mutual interference among the

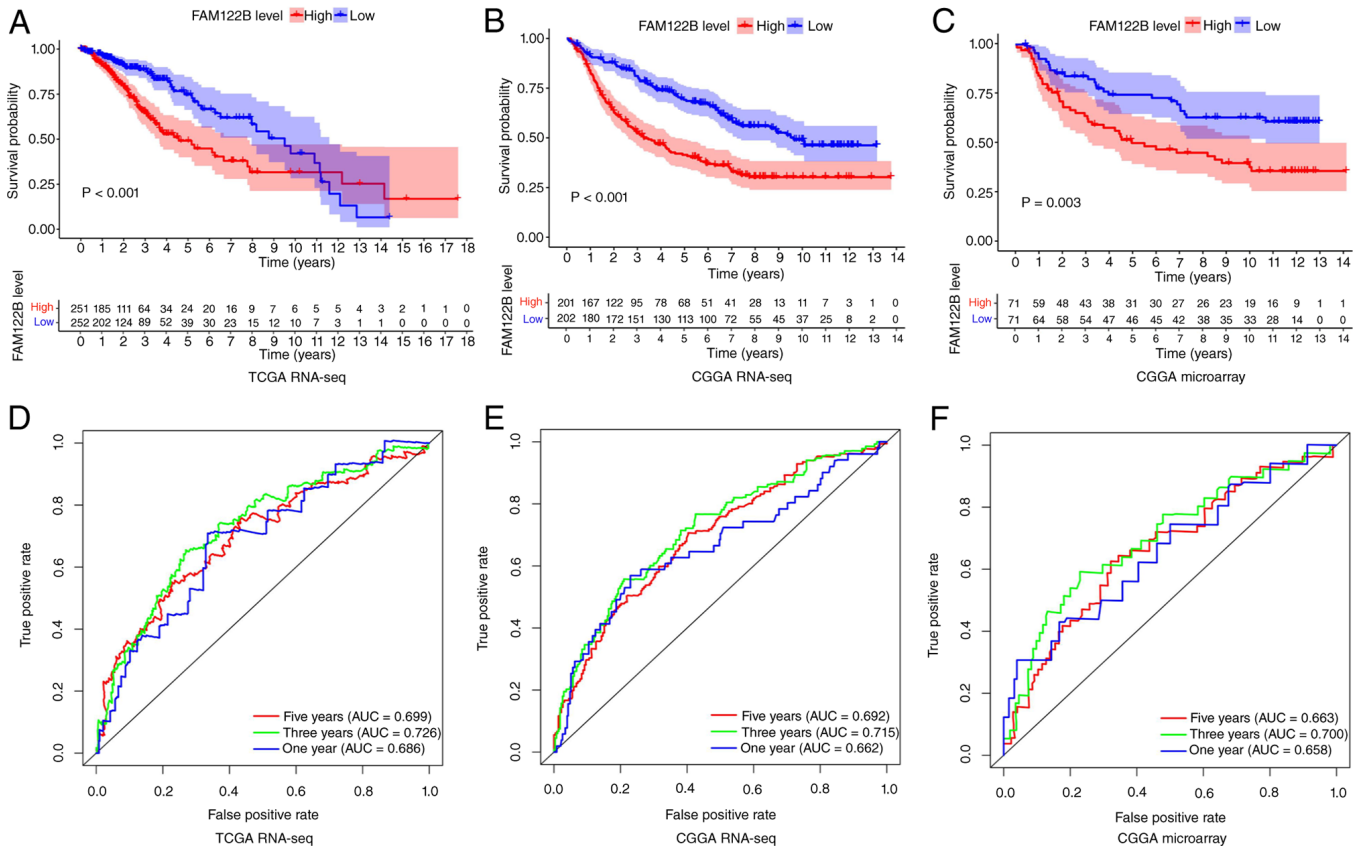

Figure 3. Prognostic value of *FAM122B* expression level in patients with LGG. (A) Kaplan-Meier survival curves of patients with LGG stratified by *FAM122B* expression levels based on TCGA RNA-seq dataset. (B) Kaplan-Meier survival curves of patients with LGG stratified by *FAM122B* expression levels based on CGGA RNA-seq dataset. (C) Kaplan-Meier survival curves of patients with LGG stratified by *FAM122B* expression levels based on CGGA microarray dataset. (D) ROC curves and AUC values of *FAM122B* for predicting 1-, 3- and 5-year survival outcomes of patients with LGG based on the TCGA RNA-seq dataset. (E) ROC curves and AUC values of *FAM122B* for predicting 1-, 3- and 5-year survival outcomes of patients with LGG based on the CGGA RNA-seq dataset. (F) ROC curves and AUC values of *FAM122B* for predicting 1-, 3- and 5-year survival outcomes of patients with LGG based on the CGGA microarray dataset. *FAM122B*, Family with sequence similarity 122, member B; LGG, low-grade glioma; TCGA, The Cancer Genome Atlas; CGGA, Chinese Glioma Genome Atlas; ROC, plot receiver operating characteristic; AUC, area under the curve.

various indicators. The results showed that across all three databases, only high *FAM122B* expression and elevated WHO grade were independent prognostic factors for poor prognosis in patients with LGG (Fig. 4B, D and F). Finally, the results of the meta-analysis across multiple datasets (HR, 1.56; 95% CI, 1.17-2.08) also indicated that *FAM122B* is a risk factor for poor prognosis in patients with LGG (Fig. 4G). In conclusion, the independent prognostic value of *FAM122B* in LGG was clarified, which lays an important theoretical foundation for subsequent in-depth exploration of the molecular regulatory mechanisms of *FAM122B*, and also provides a potential target for LGG prognosis evaluation and targeted therapy.

Co-expression analysis and GSEA of FAM122B. The occurrence and development of tumors typically involve multi-gene synergistic regulatory networks (21). To further clarify the mechanism underlying the role of *FAM122B* in the pathological progression of LGG, the present study performed co-expressed gene screening and analysis of *FAM122B* based on TCGA database. The top five genes with the strongest positive correlation with *FAM122B* were identified as *BRCC3*, *RPAP3*, *SLF1*, *MSH2* and *PHTF1*, while the top five genes with the strongest negative correlation were *MSRB2*, *MRPS28*, *APOE*, *LAMTOR1* and *PEA15* (Fig. 5A and B). Combined with information from the literature review, it was found that among the positively correlated genes, *BRCC3*, *SLF1* and *MSH2* have all been reported as oncogenes involved in tumorigenesis and progression (22-24). By contrast, *LAMTOR1* and *PEA15* are among the negatively correlated genes which have been confirmed to exert tumor-suppressive functions (25,26). The correlation between the aforementioned co-expression analysis results and genes with established functions further corroborates the potential oncogenic properties of *FAM122B* in LGG.

To clarify the specific molecular pathways through which *FAM122B* regulates the malignant progression of LGG, GSEA was performed. The results showed that the samples in the *FAM122B* high-expression group were markedly enriched in the extracellular matrix (ECM)-receptor interaction pathway, Toll-like receptor pathway and focal adhesion (Fig. 5C-E). Moreover, FDR <0.25 and P<0.05 was noted for all enriched pathways (Fig. 5F). Previous studies have confirmed that the aforementioned pathways are closely associated with tumor cell proliferation, invasion and metastasis, as well as the remodeling of the tumor immune microenvironment (27-29). Accordingly, it was suggested that *FAM122B* may regulate the

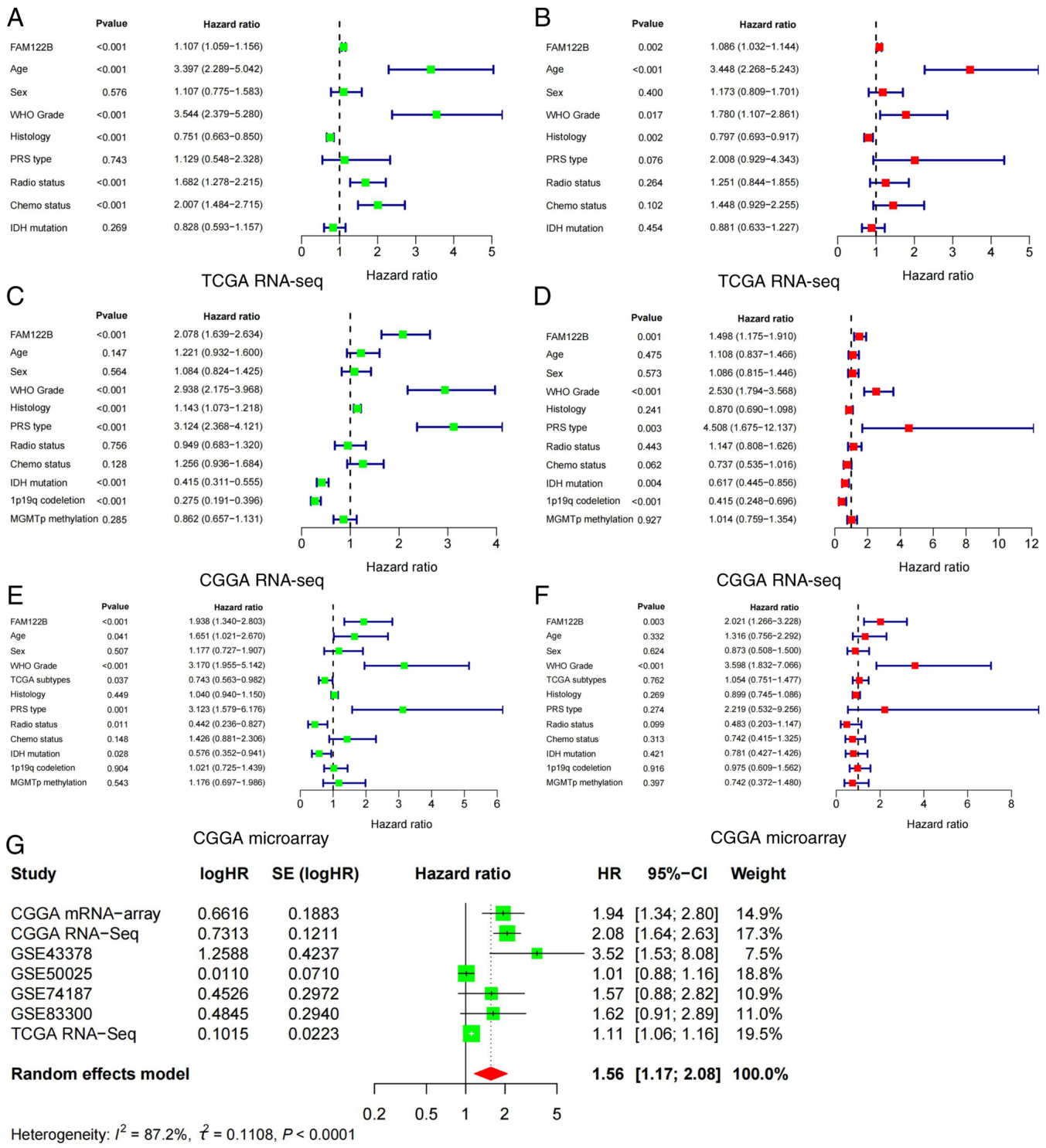

Figure 4. Validation of *FAM122B* as an independent poor prognostic factor in patients with LGG. (A) Forest plots of univariate Cox proportional hazards regression analysis based on TCGA RNA-seq dataset. (B) Forest plots of multivariate Cox proportional hazards regression analysis based on the TCGA RNA-seq dataset. (C) Forest plots of univariate Cox proportional hazards regression analysis based on CGGA RNA-seq dataset. (D) Forest plots of multivariate Cox proportional hazards regression analysis based on the CGGA RNA-seq dataset. (E) Forest plots of univariate Cox proportional hazards regression analysis based on CGGA microarray dataset. (F) Forest plots of multivariate Cox proportional hazards regression analysis based on the CGGA microarray dataset. (G) Forest plot of meta-analysis across multiple datasets, comprehensively evaluating the prognostic HR and 95% CI of *FAM122B* in patients with LGG. *FAM122B*, Family with sequence similarity 122, member B; LGG, low-grade glioma; TCGA, The Cancer Genome Atlas; CGGA, Chinese Glioma Genome Atlas; HR, hazard ratio; CI, confidence interval.

activity of these key pathways either positively or negatively, thereby affecting the malignant biological behaviors of LGG, which provides an important direction for further elucidating its molecular regulatory mechanisms.

Regulatory effect of FAM122B high expression on the immune microenvironment of LGG. To elucidate the specific mechanism through which high *FAM122B* expression modulates the malignant biological behaviors of LGG,

A

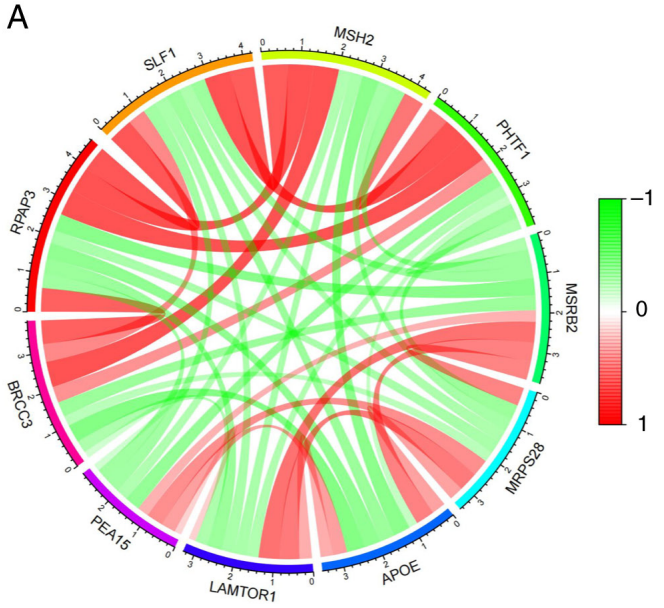

B

Gene	Correlation coefficient	P-value
MSRB2	−0.435	7.71E-26
MRPS28	−0.433	1.54E-25
APOE	−0.421	3.93E-24
LAMTOR1	−0.407	1.49E-22
PEA15	−0.404	3.39E-22
BRCC3	0.657	1.41E-66
RPAP3	0.621	9.07E-58
SLF1	0.616	1.21E-56
MSH2	0.596	2.93E-52
PHTF1	0.583	1.72E-49

C

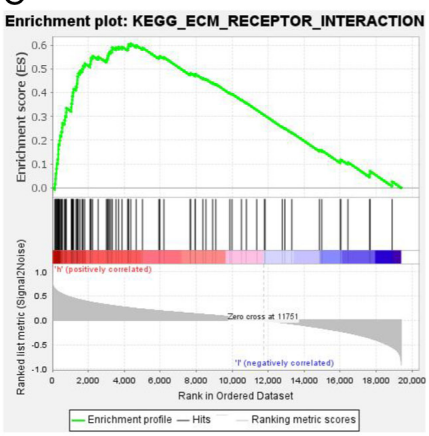

D

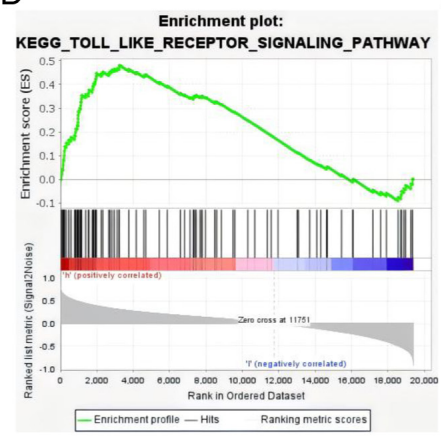

E

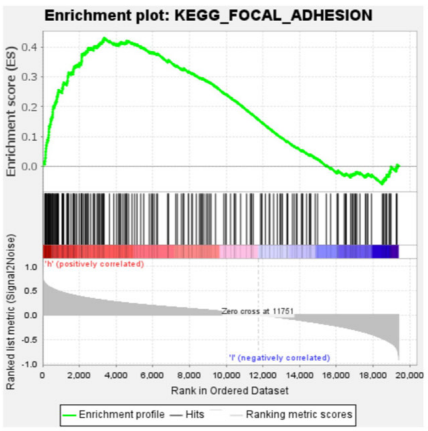

F

Pathway	ECM Receptor	Toll Like Receptor	Focal Adhesion
FDR q-value	0.104	0.119	0.131
P-value	0.012	0.035	0.048

Figure 5. Co-expression gene analysis and GSEA of *FAM122B*. (A) Chord diagram of *FAM122B* co-expressed genes, where red indicates positive correlation and green indicates negative correlation; color intensity reflects the magnitude of the correlation coefficient. (B) The top five positively and top five negatively correlated genes with *FAM122B*, along with their correlation coefficients and P-values. (C) GSEA enrichment plots showing the enrichment of extracellular matrix receptor interaction pathway in *FAM122B* high-expression samples. (D) GSEA enrichment plots showing the enrichment of Toll-like receptor signaling pathway in *FAM122B* high-expression samples. (E) GSEA enrichment plots showing the enrichment of focal adhesion pathway in *FAM122B* high-expression samples. (F) Statistical results of FDR q-values and P-values for each enriched pathway. GSEA, gene set enrichment analysis; *FAM122B*, Family with sequence similarity 122, member B; FDR, false discovery rate.

first, the ESTIMATE algorithm was employed to calculate the TME scores of patients with LGG stratified into high and low *FAM122B* expression groups. The results demonstrated that a statistically significant difference existed exclusively in the immune score between the two groups (Fig. 6A). This finding suggested that *FAM122B* may participate in the remodeling of the LGG immune microenvironment by regulating immune cell infiltration. Second, analysis of immune cell subset scatter plots revealed that the expression level of *FAM122B* may correlate with the infiltration levels of memory $CD4^+$ T cells, M2-type macrophages, activated natural killer cells and monocytes (Fig. 6B). It was therefore hypothesized that *FAM122B* may reshape the immune microenvironment by regulating changes in the distribution of these immune cell subsets, thereby promoting the malignant progression of LGG. Subsequently, the correlation between *FAM122B* expression and immune cell infiltration was explored using the TIMER database. The results showed that only $CD8^+$ T cells were positively correlated with *FAM122B* expression (Fig. S3A).

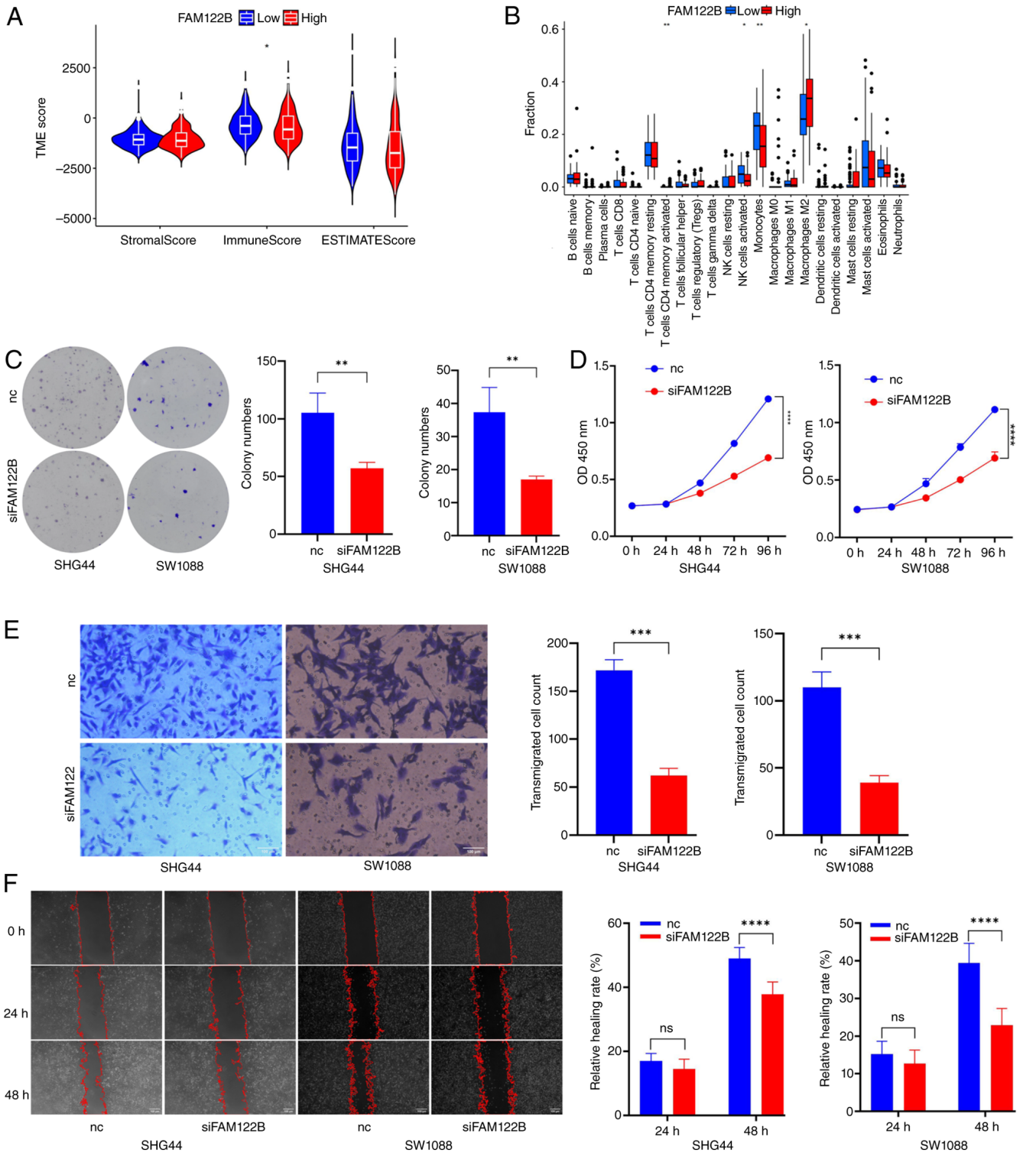

Figure 6. *FAM122B* affects LGG immune microenvironment and malignant cell behaviors. (A) TME scores of patients with LGG in *FAM122B* high- and low-expression groups, calculated by the ESTIMATE algorithm. (B) Correlation analysis between *FAM122B* expression level and infiltration levels. (C) Colony formation assay to detect the proliferation capacity of SHG44 and SW1088 cells after *FAM122B* knockdown. (D) CCK-8 assay to detect the proliferation viability of SHG44 and SW1088 cells after *FAM122B* knockdown. (E) Transwell assay to detect the invasion capacity of SHG44 and SW1088 cells after *FAM122B* knockdown. Scale bar, 100 μm. (F) Wound healing assay to detect the migration capacity of SHG44 and SW1088 cells after *FAM122B* knockdown. Scale bar, 100 μm. *P<0.05, **P<0.01, ***P<0.001, ****P<0.0001. *FAM122B*, Family with sequence similarity 122, member B; LGG, low-grade glioma; TME, tumor microenvironment; ns, no significance; si, short interfering; LGG, low-grade glioma.

Moreover, survival analysis indicated that high expression of both CD8^{+} T cells and *FAM122B* markedly shortened the overall survival of patients with LGG (Fig. S3B), suggesting that the two may synergistically affect patient prognosis. Immune checkpoints play a pivotal role in tumor immune escape and immunotherapy (30). Based on TCGA database, Spearman correlation analysis was performed to investigate the expression correlation between *FAM122B* and

classical immune checkpoint molecules (CD274, CTLA4, HAVCR2, CD96, KLRB1 and IDO1). The results showed that *FAM122B* was positively correlated with most of these immune checkpoint molecules, among which the correlation coefficient with CD274 was the highest (Table SII). As the primary ligand for programmed cell death protein 1 (PD-1), CD274 can mediate tumor cells to escape immune system attacks (31). Collectively, these bioinformatics analyses suggest that *FAM122B* may regulate the progression of LGG via participating in the remodeling of tumor immune microenvironment, which indicates that it may serve as a promising candidate target for immunotherapy of LGG.

In vitro experimental verification of the biological effects of FAM122B on LGG cells. Following the aforementioned comprehensive analyses, it was found that *FAM122B* can affect multiple biological processes of glioma. However, bioinformatics analysis alone cannot completely avoid potential false-positive results. To ensure the rigor of the present research, *in vitro* cell experiments were performed to explore the effects of *FAM122B* expression on the proliferation and migration abilities of the LGG cell lines, SHG44 and SW1088. siRNA was used to specifically knockdown *FAM122B* expression in cell lines SHG44 and SW1088 (Fig. S3C). As shown in Fig. 6C, silencing *FAM122B* markedly inhibited the colony-forming ability of LGG cell lines SHG44 and SW1088. In addition, the CCK-8 assay results showed that knocking down *FAM122B* markedly reduced the cell proliferation rate, with the difference gradually widening over time (Fig. 6D). Furthermore, the Transwell migration assay demonstrated that silencing *FAM122B* markedly decreased the number of cells migrating through the chamber (Fig. 6E). Finally, the wound healing assay further confirmed that the relative healing rate in the si*FAM122B* group was markedly lower than that in the control group at 48 h (Fig. 6F). Collectively, these results suggest that silencing *FAM122B* markedly inhibits the proliferation and migration abilities of LGG cells, further corroborating the database analysis indicating that *FAM122B* functions as an oncogene.

Discussion

Glioma is the most common malignant tumor in the central nervous system (32). As an important subtype of glioma, LGG carries a lower degree of malignancy than GBM, yet it exhibits a high risk of malignant progression and recurrence (33), posing a notable threat to the lives, health and quality of life of patients. Exploring tumor-specific biomarkers and their regulatory mechanisms is the key to breaking through the therapeutic bottleneck of LGG. In the present study, the expression pattern, clinical importance and biological functions of *FAM122B* in LGG were systematically investigated through a combination of bioinformatics analysis and *in vitro* experiments.

The FAM122 is a group of highly conserved endogenous inhibitors of PP2A, whose members are involved in diverse physiological and pathological processes by regulating PP2A activity (9). As a core member of this family, the oncogenic role of *FAM122A* has been validated by numerous studies (10,11,34). *FAM122A* can regulate biological behaviors of tumor cells including proliferation, apoptosis and invasion in various malignant tumors such as acute myeloid leukemia and hepatocellular carcinoma by inhibiting PP2A activity (9), thus exerting a key oncogenic role. However, the biological function and regulatory mechanisms of *FAM122B*, another member of the FAM122 family, in tumors remain unclear, and its role in glioma in particular has not been systematically investigated.

In the present study, the expression characteristics of *FAM122B* in LGG were first clarified through multi-dimensional verification. Based on the GEO database and LGG cell lines, it was verified that the mRNA level of *FAM122B* was markedly upregulated. In addition, IHC data of cerebral cortex and LGG tissues from the HPA database demonstrated that *FAM122B* protein expression was also markedly increased, indicating that high expression of *FAM122B* in LGG is a consistent feature at both transcriptional and translational levels, laying a foundation for the subsequent investigation of its biological functions.

To clarify the correlation between high *FAM122B* expression and the clinical characteristics as well as prognosis of LGG, the present study integrated mRNA expression data and clinical information from three databases (TCGA-seq, CGGA-seq and CGGA microarray) for comprehensive analysis. The results revealed that *FAM122B* expression was closely associated with multiple clinical phenotypes of LGG. Specifically, the expression of *FAM122B* was markedly upregulated with the elevation of WHO grade and the expression level of *FAM122B* was higher in recurrent LGG than in primary LGG. At the level of key molecular markers, *FAM122B* expression was markedly decreased in patients with LGG with an IDH mutation and 1p19q chromosomal codeletion, both of which are well-recognized favorable prognostic indicators for LGG (35). Therefore, high expression of *FAM122B* is associated with a poor prognostic phenotype, preliminarily suggesting that it may be involved in driving the malignant progression of LGG.

The ability to serve as a tumor prognostic marker largely depends on its prognostic predictive power. In the present study, Kaplan-Meier survival analysis showed that patients with high *FAM122B* expression exhibited markedly shorter survival across three independent databases, confirming the negative correlation between *FAM122B* expression and patient prognosis. ROC curve analysis further demonstrated that *FAM122B* exhibited moderate predictive value for 1-, 3- and 5-year survival in patients with LGG. The AUC remained at ~0.7, suggesting that the expression level of *FAM122B* alone has fair predictive potential for the short- to medium-term prognosis of patients with LGG. However, univariate survival analysis alone cannot exclude the interference of confounding factors such as age, pathological grade and recurrence status. Therefore, the present study further performed univariate and multivariate Cox regression analyses. The results demonstrated that after adjusting for other clinical factors, high expression of *FAM122B* and elevated WHO grade were independent adverse risk factors for patients with LGG. Based on the aforementioned analyses, it was hypothesized that *FAM122B* may mediate the malignant biological behaviors of glioma.

In the present study, three independent datasets were analyzed separately rather than being merged and integrated,

which effectively avoided the difficulty of normalization among multiple datasets. This approach not only maintained the independence of each analytical dataset, but also enabled mutual verification among the three datasets, fully demonstrating the reliability of the findings. On this basis, four additional datasets from different sources were further incorporated to perform a meta-analysis together with the original core data, thereby improving the reliability and general applicability of the research conclusions.

Although multiple independent datasets and analytical methods were included in the present study, and the corresponding results were well mutually validated, the overall analysis remains based on retrospective bioinformatic data. Retrospective research inevitably has inherent limitations and relevant biases cannot be completely avoided (36). Therefore, *in vitro* experiments were performed by selecting two LGG cell lines to explore the effects of *FAM122B* knockdown on the biological behaviors of tumor cells. The results showed that knocking down *FAM122B* markedly inhibited the proliferation and migration of both LGG cell lines, which further indicated that *FAM122B* is involved in regulating tumor malignant phenotypes and verified the reliability of the conclusions.

As overexpression experiments were not carried out in the present study, follow-up studies should add such experiments to further validate the functional role of *FAM122B*. Malignant tumor progression is a complex process involving the coordinated regulation of multiple genes and pathway disorders (37). To further explore the potential oncogenic role of *FAM122B* in LGG, the present study first performed co-expressed gene screening and analysis for *FAM122B* based on TCGA database. The results showed that the top five genes with the strongest positive correlation with *FAM122B* were *BRCC3*, *RPAP3*, *SLF1*, *MSH2* and *PHTF1*. According to the literature review, several of these genes have been confirmed to possess distinct pro-tumor functions. Specifically, *BRCC3* markedly promotes the proliferation, migration and invasion of cancer cells in various tumors, including bladder cancer (22), breast cancer (38), cervical cancer (39), pancreatic cancer (40) and colon cancer (41). In addition, as a mismatch repair protein, *MSH2* plays a crucial role in the drug resistance mechanisms of multiple cancers such as bladder cancer (24) and lung cancer (42). Furthermore, serving as a predictive indicator, *SLF1* can reflect the sensitivity of patients with colon cancer to oxaliplatin chemotherapy (23). By contrast, among the genes negatively correlated with *FAM122B*, deficiency of *LAMTOR1* can markedly suppress the malignant progression of bladder cancer (43) and colon cancer (44). Finally, *PEA15*, another negatively correlated gene, inhibits the epithelial-mesenchymal transition process in triple-negative breast cancer and exerts a tumor-suppressive effect. The consistent association of *FAM122B* with these established oncogenic or tumor-suppressive genes further corroborates its oncogenic potential in LGG, suggesting that *FAM122B* may form a synergistic regulatory network with these genes to jointly drive the progression of LGG.

The present study adopted GSEA to explore the potential regulatory mechanisms of *FAM122B* in LGG. This method is particularly suitable for investigating gene functional mechanisms, as it does not rely on artificially set thresholds for screening differentially expressed genes and thus avoids missing key regulatory genes. Moreover, it can accurately identify signaling pathways enriched with *FAM122B* at the pathway level, thereby clarifying the core molecular pathways by which *FAM122B* regulates the occurrence and progression of LGG. The results revealed that *FAM122B* was markedly enriched in three cellular signaling pathways in LGG, including ECM-receptor interaction, Toll-like receptor signaling pathway and focal adhesion. Activation of these cellular signaling pathways plays a pivotal role in tumor progression and regulates malignant phenotypes through multiple pathways and molecular mechanisms (45-47).

In the present study, indirect exploration of the biological function of *FAM122B* was attempted via the aforementioned analytical strategies. Given that the three signaling pathways exert essential regulatory effects on the formation of the immunosuppressive tumor microenvironment, the role of *FAM122B* in the immune microenvironment of LGG was further investigated. The results showed that the enrichment of tumor immune cells was markedly higher in the *FAM122B* high-expression group, particularly for M2-type tumor-associated macrophages and $CD4^+$ T cells. Meanwhile, high *FAM122B* expression was positively correlated with the levels of multiple immune checkpoint molecules.

Collectively, these findings suggest that *FAM122B* may be associated with the formation of the immunosuppressive microenvironment in LGG via the three aforementioned signaling pathways, which potentially contributes to the malignant progression of glioma. For example, glioma cells secrete abundant ECM components, such as collagen and fibronectin, which bind to surface receptors on macrophages (such as integrins, CD36 or CD44). This interaction activates downstream signaling pathways, recruiting monocytes to the tumor microenvironment and inducing their polarization into M2-type macrophages, which exhibit immunosuppressive and pro-angiogenic functions (48-50).

In glioma, abnormal activation of the Toll-like receptor signaling pathway can upregulate the expression of immune checkpoint molecules such as PD-L1, thereby enabling tumor cells to evade immune surveillance and elimination. Meanwhile, glioma further activates the TLR signaling cascade to enhance the PD-1/PD-L1 immune checkpoint pathway, which reduces the infiltration of $CD4^+$ T cells and suppresses Th1-mediated cytotoxicity within the tumor microenvironment, ultimately maintaining an overall immunosuppressive state. Furthermore, targeted intervention of the Toll-like receptor signaling pathway can effectively regulate macrophage polarization and may help reverse resistance to immune checkpoint therapy (51).

Studies have indicated that the activation of $CD4^+$ T cells is regulated by multiple factors during tumor progression (52-54). Alterations in the activity of the focal adhesion signaling pathway can modulate the function of $CD4^+$ T cells within the tumor immune microenvironment, thereby affecting the malignant progression of tumors (52). Previous literature reports also provide indirect support for these analytical findings. The present study only preliminarily explored the

biological regulatory role of *FAM122B* in the pathological progression of LGG, and its specific molecular mechanisms remain to be further verified by experiments.

The major strengths of the present study lie in the full utilization of data from multiple databases to conduct highly logical and scientifically rigorous analyses. A variety of analytical tools were adopted, enabling mutual verification among the research findings. Nevertheless, there are several shortcomings. The suggested roles of *FAM122B* in signaling pathways and the immune microenvironment are based on correlational bioinformatic analyses and were not directly validated through mechanistic experiments in the present study. The present study only provided correlational analytical outcomes rather than direct conclusive results. Further attention and in-depth improvement by subsequent researchers are required in this regard and the present work merely serves as a reference basis. The present study did not perform analyses on clinical tissue samples from patients, which constitutes a limitation of the present research. In addition, significant heterogeneity was observed in this meta-analysis. The data were collected from populations across different countries and ethnic groups and the inconsistent detection methods also contributed to heterogeneity, which may affect the reliability and interpretation of the pooled results.

In summary, the results of the present study suggest that *FAM122B* is relatively highly expressed in LGG and may act as a potential oncogene in LGG. The present study may partially fill the research gap related to the FAM122 family in LGG and help enrich the pathophysiological regulatory network of the FAM122 protein family. The present study provided preliminary evidence supporting a potential role of *FAM122B* in LGG and that further experimental and clinical studies are required to validate its clinical significance.

Acknowledgements

Not applicable.

Funding

The present study was supported by Henan Provincial Key Research and Development Program (grant no. 251111312600) and Henan Young and Middle-aged Health Science and Technology Innovation Talent Project (grant no. LJRC2023007).

Availability of data and materials

The data generated in the present study may be requested from the corresponding author.

Authors' contributions

HW was responsible for data collection and manuscript drafting. YZ participated in data collection. TG and YG were responsible for data analysis. RQ participated in study conception and experimental design, critical revision of the manuscript, project review and supervision, and funding acquisition. HW and RQ confirm the authenticity of all the raw data. All authors have read and approved the final version of the manuscript.

Ethics approval and consent to participate

Not applicable.

Patient consent for publication

Not applicable.

Competing interests

The authors declare that they have no competing interests.

References

1. Patel SH, Poisson LM, Brat DJ, Zhou Y, Cooper L, Snuderl M, Thomas C, Franceschi AM, Griffith B, Flanders AE, *et al*: T2-FLAIR mismatch, an imaging biomarker for IDH and 1p/19q status in lower-grade gliomas: A TCGA/TCIA project. Clin Cancer Res 23: 6078-6085, 2017.
2. Louis DN, Perry A, Wesseling P, Brat DJ, Cree IA, Figarella-Branger D, Hawkins C, Ng HK, Pfister SM, Reifenberger G, *et al*: The 2021 WHO classification of tumors of the central nervous system: A summary. Neuro Oncol 23: 1231-1251, 2021.
3. Jooma R, Waqas M and Khan I: Diffuse Low-grade glioma-changing concepts in diagnosis and management: A review. Asian J Neurosurg 14: 356-363, 2019.
4. Nahed BV, Redjal N, Brat DJ, Chi AS, Oh K, Batchelor TT, Ryken TC, Kalkanis SN and Olson JJ: Management of patients with recurrence of diffuse low grade glioma: A systematic review and evidence-based clinical practice guideline. J Neurooncol 125: 609-630, 2015.
5. Fournier C, Mercey-Ressejac M, Derangère V, Al Kadi A, Rageot D, Charrat C, Leroy A, Vollaire J, Josserand V, Escudé M, *et al*: Nanostructured lipid carriers based mRNA vaccine leads to a T cell-inflamed tumour microenvironment favourable for improving PD-1/PD-L1 blocking therapy and long-term immunity in a cold tumour model. EBioMedicine 112: 105543, 2025.
6. Sun X, Jia Q, Li K, Tian C, Yi L, Yan L, Zheng J, Jia X and Gu M: Comparative genomic landscape of lower-grade glioma and glioblastoma. PLoS One 19: e0309536, 2024.
7. Yang YS, Liu MH, Yan ZW, Chen GQ and Huang Y: FAM122A is required for mesendodermal and cardiac differentiation of embryonic stem cells. Stem Cells 41: 354-367, 2023.
8. Fan F, Zhao J, Liu Y, Zhao H, Weng L, Li Q, Chen G and Xu Y: Identifying the SUMO1 modification of FAM122A leading to the degradation of PP2A-Cα by ubiquitin-proteasome system. Biochem Biophys Res Commun 500: 676-681, 2018.
9. Wasserman JS, Faezov B, Patel KR, Kurimchak AM, Palacio SM, Glass DJ, Fowle H, McEwan BC, Xu Q, Zhao Z, *et al*: FAM122A ensures cell cycle interphase progression and checkpoint control by inhibiting B55α/PP2A through helical motifs. Nat Commun 15: 5776, 2024.
10. Liu MH, Chen J, Yang YS, Wang YQ, Chen GQ, Zhang Y and Huang Y: FAM122A promotes acute myeloid leukemia cell growth through inhibiting PP2A activity and sustaining MYC expression. Haematologica 106: 903-907, 2021.
11. Zhou Y, Shi WY, He W, Yan ZW, Liu MH, Chen J, Yang YS, Wang YQ, Chen GQ and Huang Y: FAM122A supports the growth of hepatocellular carcinoma cells and its deletion enhances Doxorubicin-induced cytotoxicity. Exp Cell Res 387: 111714, 2020.
12. Livak KJ and Schmittgen TD: Analysis of relative gene expression data using real-time quantitative PCR and the 2(-Delta Delta C(T)) method. Methods 25: 402-408, 2001.
13. Kawaguchi A, Yajima N, Tsuchiya N, Homma J, Sano M, Natsumeda M, Takahashi H, Fujii Y, Kakuma T and Yamanaka R: Gene expression signature-based prognostic risk score in patients with glioblastoma. Cancer Sci 104: 1205-1210, 2013.
14. Buczkowicz P, Hoeman C, Rakopoulos P, Pajovic S, Letourneau L, Dzamba M, Morrison A, Lewis P, Bouffet E, Bartels U, *et al*: Genomic analysis of diffuse intrinsic pontine gliomas identifies three molecular subgroups and recurrent activating ACVR1 mutations. Nat Genet 46: 451-456, 2014.

15. Yu X, Feng L, Liu D, Zhang L, Wu B, Jiang W, Han Z and Cheng S: Quantitative proteomics reveals the novel co-expression signatures in early brain development for prognosis of glioblastoma multiforme. Oncotarget 7: 14161-14171, 2016.
16. Feng L, Qian H, Yu X, Liu K, Xiao T, Zhang C, Kuang M, Cheng S, Li X, Wan J and Zhang K: Heterogeneity of tumor-infiltrating lymphocytes ascribed to local immune status rather than neoantigens by multi-omics analysis of glioblastoma multiforme. Sci Rep 7: 6968, 2017.
17. Park CK, Park I, Lee S, Sun CH, Koh Y, Park SH, Kim JE, Yun H and Lee SH: Genomic dynamics associated with malignant transformation in IDH1 mutated gliomas. Oncotarget 6: 43653-43666, 2015.
18. Björkblom B, Wibom C, Eriksson M, Bergenheim AT, Sjöberg RL, Jonsson P, Brännström T, Antti H, Sandström M and Melin B: Distinct metabolic hallmarks of WHO classified adult glioma subtypes. Neuro Oncol 24: 1454-1468, 2022.
19. Chen W, Lei C, Liu P, Liu Y, Guo X, Kong Z, Wang Y, Dai C, Wang Y, Ma W and Wang Y: Progress and prospects of recurrent glioma: A recent scientometric analysis of the web of science in 2019. World Neurosurg 134: e387-e399, 2020.
20. Decuyper M, Bonte S, Deblaere K and Van Holen R: Automated MRI based pipeline for segmentation and prediction of grade, IDH mutation and 1p19q co-deletion in glioma. Comput Med Imaging Graph 88: 101831, 2021.
21. Huang S, Ernberg I and Kauffman S: Cancer attractors: A systems view of tumors from a gene network dynamics and developmental perspective. Semin Cell Dev Biol 20: 869-876, 2009.
22. Tao H, Liao Y, Yan Y, He Z, Zhou J, Wang X, Peng J, Li S and Liu T: BRCC3 promotes tumorigenesis of bladder cancer by activating the NF-κB signaling pathway through targeting TRAF2. Front Cell Dev Biol 9: 720349, 2021.
23. Han X, Wang Z, Zhang L, Shen Y, Tan Q, Sun Y, Wang J, Qian X, Yang H and Shi Y: SLF1 polymorphism predicts response to oxaliplatin-based adjuvant chemotherapy in patients with colon cancer. Am J Cancer Res 11: 1522-1539, 2021.
24. Zhang H, Xiao X, Wei W, Huang C, Wang M, Wang L, He Y, Sun J, Jiang Y, Jiang G and Zhang X: CircLIFR synergizes with MSH2 to attenuate chemoresistance via MutSα/ATM-p73 axis in bladder cancer. Mol Cancer 20: 70, 2021.
25. Wu B, Huang X, Shi X, Jiang M, Liu H and Zhao L: LAMTOR1 decreased exosomal PD-L1 to enhance immunotherapy efficacy in non-small cell lung cancer. Mol Cancer 23: 184, 2024.
26. Mohammed HN, Pickard MR and Mourtada-Maarabouni M: The protein phosphatase 4-PEA15 axis regulates the survival of breast cancer cells. Cell Signal 28: 1389-1400, 2016.
27. Neophytou CM, Panagi M, Stylianopoulos T and Papageorgis P: The role of tumor microenvironment in cancer metastasis: Molecular mechanisms and therapeutic opportunities. Cancers 13: 2053, 2021.
28. Zhang P, Cao X, Guan M, Li D, Xiang H, Peng Q, Zhou Y, Weng C, Fang X, Liu X, *et al*: CPNE8 promotes gastric cancer metastasis by modulating focal adhesion pathway and tumor microenvironment. Int J Biol Sci 18: 4932-4949, 2022.
29. Benencia F, Alaniz LD and McCall KD: Editorial: Toll-like receptor expression in transformed cells: Role in tumor development and cancer therapies. Front Immunol 15: 1478431, 2024.
30. Mortezaee K: Immune escape: A critical hallmark in solid tumors. Life Sci 258: 118110, 2020.
31. Pardoll DM: The blockade of immune checkpoints in cancer immunotherapy. Nat Rev Cancer 12: 252-264, 2012.
32. Ostrom QT, Price M, Neff C, Cioffi G, Waite KA, Kruchko C and Barnholtz-Sloan JS: CBTRUS statistical report: Primary brain and other central nervous system tumors diagnosed in the United States in 2015-2019. Neuro Oncol 24 (Suppl 5): v1-v95, 2022.
33. Nakasu S and Nakasu Y: Malignant progression of diffuse Low-grade Gliomas: A systematic review and Meta-analysis on incidence and related factors. Neurol Med Chir (Tokyo) 62: 177-185, 2022.
34. Wang YQ, Yang YS, Chen J, Liu MH, Chen GQ and Huang Y: FAM122A maintains DNA stability possibly through the regulation of topoisomerase IIα expression. Exp Cell Res 396: 112242, 2020.
35. Familiari P, Lapolla P, Picotti V, Palmieri M, Pesce A, Carosi G, Relucenti M, Nottola S, Gianno F, Minasi S, *et al*: Role of 1p/19q codeletion in diffuse Low-grade glioma tumour prognosis. Anticancer Res 43: 2659-2670, 2023.
36. Talari K and Goyal M: Retrospective studies-utility and caveats. J R Coll Physicians Edinb 50: 398-402, 2020.
37. Charmpi K, Guo T, Zhong Q, Wagner U, Sun R, Toussaint NC, Fritz CE, Yuan C, Chen H, Rupp NJ, *et al*: Convergent network effects along the axis of gene expression during prostate cancer progression. Genome Biol 21: 302, 2020.
38. Huang Q, Zheng S, Gu H, Yang Z, Lu Y, Yu X and Guo G: The deubiquitinase BRCC3 increases the stability of ZEB1 and promotes the proliferation and metastasis of triple-negative breast cancer cells. Acta Biochim Biophys Sin (Shanghai) 56: 564-575, 2024.
39. Zhang F and Zhou Q: Knockdown of BRCC3 exerts an anti-tumor effect on cervical cancer *in vitro*. Mol Med Rep 18: 4886-4894, 2018.
40. Hu X, Wu J and Xu J: UCA1 executes an oncogenic role in pancreatic cancer by regulating miR-582-5p/BRCC3. Front Oncol 13: 1133200, 2023.
41. Feng X, He S, Chen Y and Zhang L: Deubiquitinase BRCC3 promotes the migration, invasion and EMT progression of colon adenocarcinoma by stabilizing MET expression. Genes Genomics 46: 637-646, 2024.
42. Ko JC, Chiu HC, Wo TY, Huang YJ, Tseng SC, Huang YC, Chen HJ, Syu JJ, Chen CY, Jian YT, *et al*: Inhibition of p38 MAPK-dependent MutS homologue-2 (MSH2) expression by metformin enhances gefitinib-induced cytotoxicity in human squamous lung cancer cells. Lung Cancer 82: 397-406, 2013.
43. Sun Y, Guan Z, Sheng Q, Duan W, Zhao H, Zhou J, Deng Q and Pei X: N-myristoyltransferase-1 deficiency blocks myristoylation of LAMTOR1 and inhibits bladder cancer progression. Cancer Lett 529: 126-138, 2022.
44. Zhao L, Gao N, Peng X, Chen L, Meng T, Jiang C, Jin J, Zhang J, Duan Q, Tian H, *et al*: TRAF4-mediated LAMTOR1 ubiquitination promotes mTORC1 activation and inhibits the inflammation-induced colorectal cancer progression. Adv Sci (Weinh) 11: e2301164, 2024.
45. Kidd LC, Rogers EN, Yeyeodu ST, Jones DZ and Kimbro KS: Contribution of toll-like receptor signaling pathways to breast tumorigenesis and treatment. Br Cancer (Dove Med Press) 5: 43-51, 2013.
46. Liu Z, Zhang X, Ben T, Li M, Jin Y, Wang T and Song Y: Focal adhesion in the tumour metastasis: From molecular mechanisms to therapeutic targets. Biomark Res 13: 38, 2025.
47. Lu P, Weaver VM and Werb Z: The extracellular matrix: A dynamic niche in cancer progression. J Cell Biol 196: 395-406, 2012.
48. Cui X, Morales RT, Qian W, Wang H, Gagner JP, Dolgalev I, Placantonakis D, Zagzag D, Cimmino L, Snuderl M, *et al*: Hacking macrophage-associated immunosuppression for regulating glioblastoma angiogenesis. Biomaterials 161: 164-178, 2018.
49. Xiong J, Xiao R, Zhao J, Zhao Q, Luo M, Li F, Zhang W and Wu M: Matrix stiffness affects tumor-associated macrophage functional polarization and its potential in tumor therapy. J Transl Med 22: 85, 2024.
50. Ellert-Miklaszewska A, Poleszak K, Pasierbinska M and Kaminska B: Integrin signaling in glioma pathogenesis: From biology to therapy. Int J Mol Sci 21: 888, 2020.
51. Norollahi SE, Babaei K, Rashidy-Pour A, Yousefi B, Baharlou R, Far BF, Jalali A and Samadani AA: Role of the TLR signaling pathway in the pathogenesis of glioblastoma multiforme with an emphasis on immunotherapy. Biochem Biophys Rep 43: 102149, 2025.
52. Wiemer AJ, Wernimont SA, Cung TD, Bennin DA, Beggs HE and Huttenlocher A: The focal adhesion kinase inhibitor PF-562,271 impairs primary CD4+ T cell activation. Biochem Pharmacol 86: 770-781, 2013.
53. Guo M, Liu MYR and Brooks DG: Regulation and impact of tumor-specific CD4(+) T cells in cancer and immunotherapy. Trends Immunol 45: 303-313, 2024.
54. Accogli T, Bruchard M and Végran F: Modulation of CD4 T cell response according to tumor cytokine microenvironment. Cancers 13: 373, 2021.